Ionospheric Profiling Through Radio-Frequency Signals Recorded by the FORTÉ Satellite, With Comparison to the International Reference Ionosphere

Ronald W. Moses and Abram R. Jacobson

Los Alamos National Laboratory, Los Alamos, NM 87545, USA

ABSTRACT

Radio-frequency signals originating on Earth and recorded in space allow retrieval of ionospheric parameters. Using the FORTÉ (Fast Onboard Recording of Transient Events) satellite, it has been shown that trans-ionospheric pulsed radio-frequency signals carry sufficient information to infer the peak electron density of the ionosphere, in addition to the total electron content along a ray path between a source and a receiver. In this paper the detailed refractive properties of the ionosphere and the birefringent splitting of radio-frequency waves in the Earth's magnetic field are modeled using the Appleton-Hartree equation and an electron density profile based on the International Reference Ionosphere. Applications of this model to FORTÉ data provide additional information on the vertical profile of ionospheric plasma density at the time and place of measurement. Results of the FORTÉ observations are compared with the International Reference Ionosphere.

INTRODUCTION AND BACKGROUND

Ionospheric monitoring from both Earth and space has become a well-refined science. The electron density profile can be determined from ground level up to the peak electron density using an ionosonde (Budden, 1988). Satellite borne topside sounders can determine the electron density profile above the peak density layer (Bilitza and Williamson, 1999). Trans-ionospheric signals are used to obtain the integrated electron density, called the total electron content (TEC), between a transmitter and receiver (Budden, 1988). Incoherent scatter radars probe both electron and ion properties (Kelley, 1989). Transmissions from multiple sources such as the Global Positioning System are used to create tomographic representations of ionospheric profiles (Heise, 2002).

In this paper, we build on earlier work at Los Alamos National Laboratory (Massey *et al.*, 1998; Jacobson *et al.*, 1999; and Roussel-Dupre *et al*., 2001) using trans-ionospheric pulse data recorded by the FORTÉ satellite to extract ionospheric parameters. There are several ray tracing codes such as TRACKER (Argo, *et al.*, 1992), TIPC, and ITF (Roussel-Dupre *et al*., 2001) that are used to model radio-frequency (RF) wave propagation through the dispersive plasma of the ionosphere. For the development of most of these codes, it has been assumed that the plasma frequency, f_{pe}, is considerably smaller than the wave frequency, f. Then, the index of refraction of the ionospheric plasma, n, given by the Appleton-Hartree equation (Budden, 1988) is expressed in a Taylor expansion of order up to $(f_{pe}/f)^4$. In the present work, the use of wave frequencies approaching the plasma frequency is enabled by modeling the full functional dependence on f_{pe}/f, avoiding the inherent errors in a truncated series expansion. A multi-layered ionospheric model is described as a set of concentric spherical shells of plasma. Ray paths and frequency dependent time lag are computed between a transmitter on Earth and the satellite location. The computer model is fit to FORTÉ obtained time-lag data. A model of the ionospheric electron density profile is developed by scaling to a profile example of the International Reference Ionosphere (IRI) (Bilitza, 1990). The vertically integrated total electron content, peak plasma frequency, and a scaled ionospheric thickness are extracted from the data and compared with the IRI.

Physics of Ionospheric Wave Propagation

Ionospheric electron density information can be gleaned from satellite observations as follows. The index of refraction of a plasma, n, is given in the Appleton-Hartree equation as a function of the frequency, f, of RF waves passing through the plasma (Budden, 1988)

$$n^2 = 1 - X \Big/ \left(1 - \tfrac{1}{2}Y^2 \sin^2\beta \Big/ (1-X) \pm \sqrt{\tfrac{1}{4}Y^4 \sin^4\beta \Big/ (1-X)^2 + Y^2 \cos^2\beta}\right) \tag{1}$$

where $X \equiv \left(f_{pe}/f\right)^2$, $Y \equiv f_{ce}/f$, $f_{pe}^2 = e^2 N_e \big/ \left(4\pi^2 \varepsilon_o m_e\right)$, $f_{ce} = eB/m_e$, f_{pe} is the electron plasma frequency; f_{ce} is the electron cyclotron frequency; N_e is the electron density; e is the electron charge; m_e is the electron mass; ε_o is the permittivity of free space; B is the magnitude of the local magnetic field, and β is the angle between the magnetic field vector and the direction of wave propagation. The total phase shift in radians between the transmitter, T, and receiver, R, is $\varphi = (2\pi/c)\int_T^R n(f,s)\, f\, ds$ where c is the speed of light in free space, and the integration is taken along the refracted ray path from T to R, appropriate to f. It is a well-known result of wave optics that the time required for a wave packet centered on f to go from T to R is

$$\tau(f) = \frac{1}{2\pi}\frac{\partial\varphi}{\partial f}. \tag{2}$$

This gives the same result as following a refracted ray and tracking the wave packet at the group speed,

$$v_g = \left[\frac{\partial}{\partial f}\left(\frac{fn}{c}\right)\right]^{-1}. \tag{3}$$

Extraction of Ionospheric Parameters from Propagation Time Lag

The FORTÉ satellite records time-dependent RF signals over a broad frequency range when they arise from lightning and man-made sources. Fourier analysis of the recorded data with a sliding window reveals the observed time lag of a pulsed signal as a function of frequency, $\tau(f)$. Much of the capability in utilizing FORTÉ data is described by Massey *et al.* (1998), Jacobson *et al.* (1999), and Roussel-Dupre *et al.* (2001).

Data returned from FORTÉ may be displayed as in Figure 1a, showing the functional relationship between frequency and time delay. Here, the Los Alamos Portable Pulser (LAPP), developed by Daniel Holden and colleagues, provides a ~10ns single sine wave signal from a known location (Massey *et al.*, 1998). The data recorded and returned by FORTÉ are subsequently Fourier analyzed for display as in Figure 1a. The two hyperbolic curves visible in Figure 1a arise from separation of the ordinary and extra-ordinary waves. These data have been digitized by eye as "O" and "X" points in Figure 1b, standing for the ordinary and extra-ordinary rays respectively. It is estimated that the digitization process introduces a random error of ~ 0.3μs in the horizontal positions of the points.

Now the objective is to use the physics in Eqs. (1) and (2) to develop specific ionospheric models using data such as those in Figure 1. If in fact X and Y are small compared to unity in Eq. (1), one may choose to limit consideration to a Taylor expansion of the index of refraction,

$$n \approx 1 - \frac{1}{2}\left(\frac{f_p}{f}\right)^2 + \frac{s}{2}\frac{f_p^2 f_{ce}}{f^3}\cos\beta - \frac{1}{4}\left[\frac{f_p^2}{2} + \left(2 - \sin^2\beta\right) f_{ce}^2\right]\frac{f_p^2}{f^4} + \cdots. \tag{4}$$

where $s = \pm 1$, with "+" representing ordinary waves, circularly polarized opposite to the cyclotron rotation of electrons and "-" standing for extra-ordinary waves polarized with the cyclotron rotation.

If the satellite were at a height h directly above the transmitter, the time between transmission of a wave packet centered on frequency f and reception of that wave packet would be

$$\tau(f) = \frac{h}{c} + \frac{C_2}{f^2} + \frac{sC_3}{f^3} + \frac{C_4}{f^4} + \cdots. \tag{5}$$

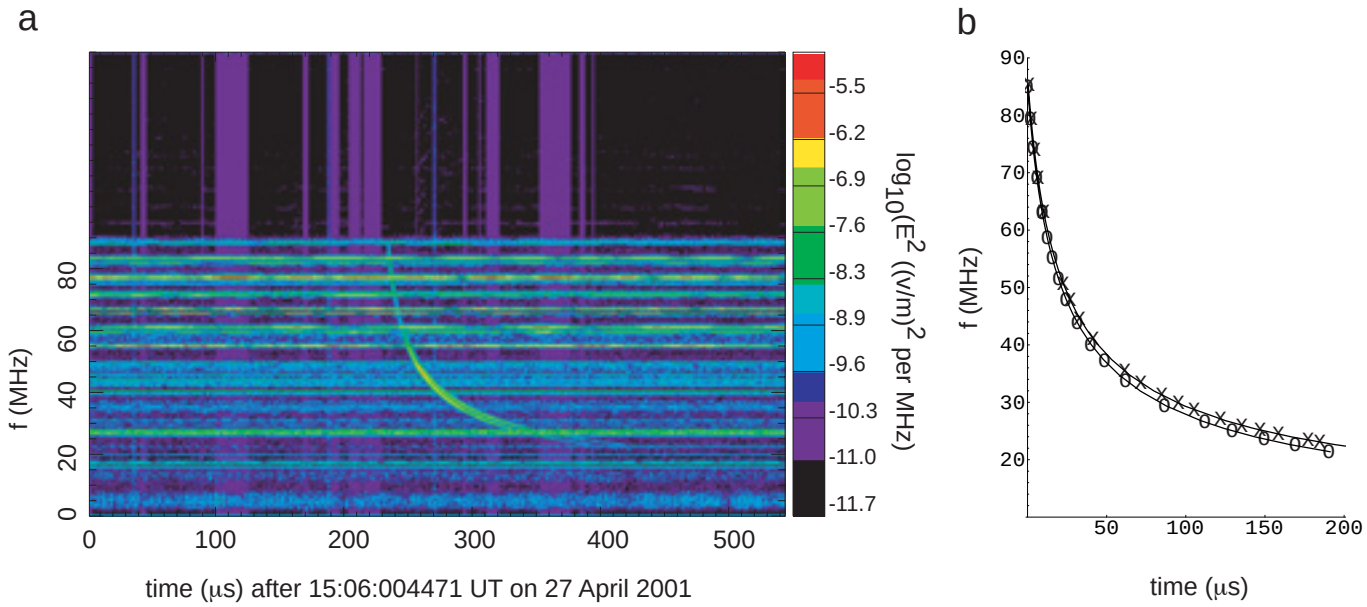

Fig. 1. Fourier analyzed data taken by the FORTÉ satellite, showing (a) the functional dependence between the central frequency of a wave packet and the time that wave packet is recorded by the satellite, and (b) the digitized frequency versus lag-time data from FORTÉ for O – ordinary and X – extra-ordinary circular polarizations. In (b) the solid curves fit to the data originate with the trans-ionospheric propagation model from which density and thickness information is extracted. The time scale in (b) has an offset zero relative to (a). The spectrum above 90 *MHz* is suppressed by a filter.

The coefficients in Eq. (5) are:

$$C_2 = \frac{e^2}{8\pi^2 c\,\varepsilon_o m_e}\int_0^h N_e(z)dz\,, \tag{6a}$$

$$C_3 = \frac{-e^3}{4\pi^2 c\,\varepsilon_o m_e^2}\int_0^h N_e(z)B(z)\cos\beta(z)dz\,, \tag{6b}$$

and

$$C_4 = \frac{3}{8c}\left[\left(\frac{e^2}{4\pi^2\varepsilon_o m_e}\right)^2\int_0^h N_e^2(z)dz + \frac{e^4}{2\pi^2\varepsilon_o m_e^3}\int_0^h N_e(z)B^2(z)\left(1+\cos^2\beta(z)\right)dz\right]. \tag{6c}$$

If FORTÉ were directly above the transmitter, one could do a least-squares fit of Eq. (5) to the data of Figure 1b to solve for C_2, C_3, and C_4. The vertical TEC is defined as the first moment of N_e and is easily extracted as

$$TEC = M_{N1} \equiv \int_0^h N_e(z)dz = \frac{8\pi^2 c\,\varepsilon_o m_e}{e^2}C_2\,. \tag{7}$$

The birefringent splitting term, C_3, will be addressed later, and the contribution of f_{ce} to C_4 is small enough to be ignored in Eq. (6c). Hence, the second moment of density is given as

$$M_{N2} \equiv \int_0^h N_e^2(z)dz = \frac{2c}{3}\left(\frac{8\pi^2\varepsilon_o m_e}{e^2}\right)^2 C_4\,. \tag{8}$$

To give meaning to information accessible from Eqs. (7) and (8) combined, let us assume that the vertical profile N_e can be characterized by a scalable shape

$$N_e = N_{eo} P\left(\left(z - z_o\right)/T\right) \tag{9}$$

where N_{eo} is the maximum electron density, z_o is the altitude of the maximum of N_e, and T is the equivalent thickness of the ionosphere (below FORTÉ) if it were of uniform density. These definitions hold when

$$1 = \int P(\xi) d\xi \tag{10}$$

with the limits of integration being in space where $P \rightarrow 0$. Considering Eqs. (7), (9), and (10) one then has

$$TEC = N_{eo} T = M_{N1}. \tag{11}$$

If in fact ionospheric density were a "rectangle" of uniform density, one would have

$$N_{eo}\, TEC = N_{eo}^2 T = M_{N2}. \tag{12a}$$

If the profile were a linear slope on either side of a single peak forming a triangle, the second moment of N_e would relate to peak density, thickness, and TEC as follows (Myre, 2002)

$$N_{eo}\, TEC = N_{eo}^2 T = 1.5\, M_{N2}. \tag{12b}$$

This simple model of a satellite at zenith shows that one can extract peak density and thickness information as well as TEC from a fourth-order expansion of time lag, but it is necessary to have additional knowledge of ionospheric profile to distinguish between Eqs. (12a) and (12b).

Next, the more general problem is solved for the satellite being significantly away from the zenith of the transmitter. Roussel-Dupre *et al.* (2001) described how the ray bending due to refraction at the edges of the ionosphere can lengthen the optical path between a radiation source and a satellite receiver for oblique incidence on the ionosphere. This functional dependence of the opticsl path length on frequency introduces a quartic term, $1/f^4$, on the right hand side of Eq. (4). When such a term enters due to geometrical optics, one must also consider the higher-order terms in the index of refraction itself, Eq. (1). Massey *et al.* (1998) modeled the ionosphere as a planar structure with a single layer of plasma having uniform density, while Roussel-Dupre *et al*. (2001) used a spherical ionospheric model. In both of these papers, a Taylor expansion through fourth order in f_{pe}/f was used to represent the frequency-dependent time lag of wave packets traversing the ionosphere. Such an approach works well, provided the satellite is close enough to the RF source to avoid the impact of higher-order terms. The purpose of this paper is to provide a full nonlinear dependence of the time lag in a model that properly represents curvature of the Earth and a density profiled ionosphere based on the IRI.

Layered Ionospheric Model

The ionospheric model used in this paper starts with a set of spherical shells, each having uniform electron density. The height, thickness, and density of each shell, as well as the number of shells are free parameters. The coordinates of the ground-based transmitter and the FORTÉ satellite are known for the time of the trans-ionospheric pulse to be modeled. The *Mathematica* code written for this model has two parts. The first part takes a specific numerical description of the ionosphere and computes the frequency-dependent time lag for pulses traveling from the transmitter to FORTÉ. Here, the line of sight between the transmitter and satellite is taken as the first estimate of the ray path. Using Eq. (1) and the International Reference Geomagnetic Field (IRGF) (Barton, 1997), the index of refraction is calculated through each layer of the model. A test ray with a specific frequency is launched from the location of the transmitter, and Snell's law is used to compute the angles of refraction at each surface interface until the test ray reaches the vicinity of the satellite. A shooting method is used to iteratively adjust the angle of launch of the test rays until a ray is computed to intersect the location of the satellite to a reasonable level of precision. When the transmitter to satellite ray path is known for a given frequency, the time lag for a pulse centered on that frequency is computed.

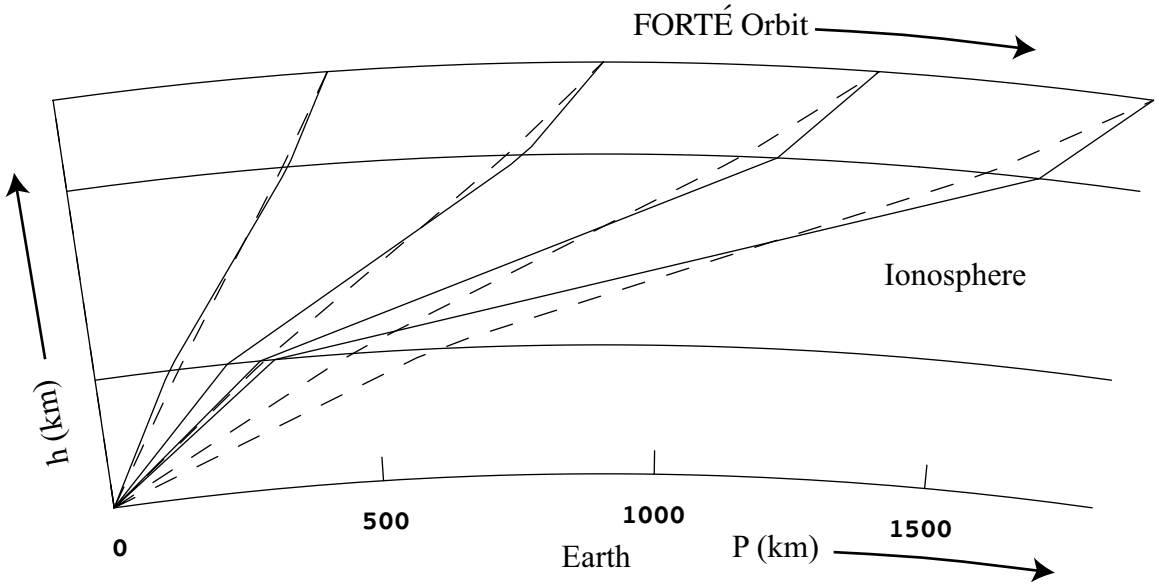

Fig. 2. Ray tracing from LAPP to FORTÉ showing refraction at the edges of a uniform density ionospheric model. The transmitter is located at the origin, the great-circle path length from the transmitter to the footprint of FORTÉ is defined as *P*, and the altitude is *h*. A 22MHz signal would follow the ray paths shown as solid lines, while a 79MHz signal would traverse the dashed lines.

For the second part of the *Mathematica* code, numerical descriptors are chosen for peak density, N_{eo}, and ionospheric thickness, T, similar to Eq. (9). Given these values, one can then tabulate a model-dependent time lag, $\tau(f)$, for each frequency in a data set such as Figure 1b. The time lag is a nonlinear function of f, N_{eo}, and T. An iterative procedure (Wolberg, 1967) is used to solve for N_{eo} and T giving a least-squares fit of $\tau(f)$ to the experimentally obtained $\tau(f)$ data.

The aforementioned approach has been used to fit an ionospheric model to FORTÉ data, inferring the thickness and density of the ionosphere as well as its vertical TEC (Moses and Jacobson, 2001). The simplest and "cleanest" source for RF illumination of a receiver aboard a satellite like FORTÉ is from a man-made, broadband pulsed source. Analysis of LAPP signals provides the data for this paper.

The modeling of a single, uniform layer ionosphere is illustrated in Figure 2 where rays are traced from a ground-based source through the ionospheric model to five possible satellite positions. The solid ray paths are for $f = 22$MHz, and the dashed paths are for $f = 79$MHz. One can see that the lower frequencies are refracted more, because $X = \left(f_{pe} / f \right)^2$ has a greater effect on the index of refraction, n, in Eq. (1). Actual data taken from analysis of signals recorded by FORTÉ are displayed in Figure 1b, where O and X represent ordinary and extra-ordinary wave polarizations respectively. The code described above was used to find the least squares fit to the data, and the respective fits for the ordinary and extra-ordinary polarizations are plotted as solid lines in Figure 1b. Using the model of a single layer ionosphere of uniform density, the nonlinear analysis allows one to estimate the ionospheric thickness to be 370 km and the plasma frequency to be $f_{pe} = 8.6$ MHz.

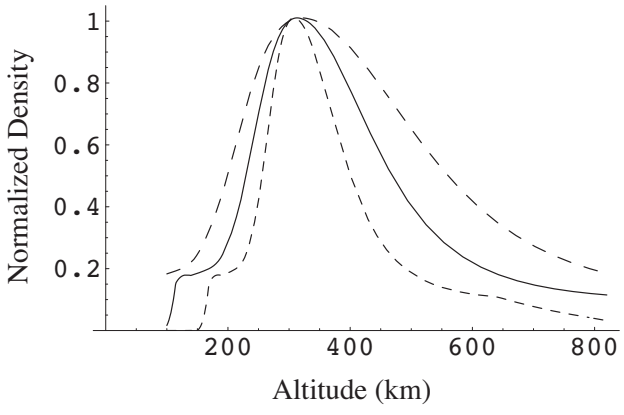

Fig. 3. The normalized vertical profile of the International Reference Ionosphere above Los Alamos, NM on April 28, 2001, at 15:16 UT is scaled to represent ionospheric thicknesses of 200 *km* (short dashed), 300 *km* (solid), and 400 *km* (long dashed). The solid curve is the closest match to the precise IRI profile thickness of 318 *km* at that place and time.

A realistic treatment of the ionosphere should not be restricted to a layer of uniform density. As demonstrated in Eq. (12), a moment expansion of time lag will give a 50% higher peak density for a triangular profile than for one that is uniform. Although there is no universal two-parameter profile such as Eq. (9) that provides a general ionospheric model, we choose to follow a widely-used profile that has been extensively validated. Here, the IRI is chosen as a template for the ionospheric profile. FORTÉ data taken on April 28, 2001 at 15:05 – 15:10 UT were chosen for the base case. The corresponding vertical profile for the IRI over Los Alamos, NM at that time and date is used as the template. This IRI profile has a width of 318 *km* when defined in accordance with Eq. (11), and its peak electron density occurs at $h \approx 300\,km$. For the purposes of this work, a numerical scaling of the IRI base case was developed whereby the peak electron density stays at 300 *km*, and the profiles above and below 300 *km* are scaled to achieve variable thickness. Figure 3 shows the scaled profile based on the IRI with thickness ranging from T = 200 to 400 *km*.

DATA ANALYSIS

Time lag data were taken for analysis from 36 FORTÉ passes within range of the LAPP transmitter. Results are considered where 4 to 8 LAPP pulses were recorded by FORTÉ. The ionospheric model described above was fit to the time lag data to extract the vertical TEC, f_{peo}, and T for each pulse. The statistical behavior of the results is examined in an effort to understand the performance of this analysis technique and the steps needed to improve it.

The data were digitized from the form seen in Figure 1a to numerical values such as those plotted as "O" and "X" points in Figure 1b. The data for each pulse are placed in a separate file including positions of the transmitter and satellite as well as the time delay and frequency data. The data files are named with a common identifier for the FORTÉ pass and a pulse number unique within that pass. The ray path from the ground to the FORTÉ satellite, at about 800 *km* altitude, was divided into 13 layers with a higher concentration of layers in the vicinity of the peak electron density, ~ 300 *km* altitude. The electron densities in these 13 layers of the model were fit to the scaled IRI profiles illustrated in Figure 3. The analysis code reads each pulse file separately, does a least-squares fit on the time-lag data, solving for N_{eo}, T, and vertical TEC in the process. The peak density, N_{eo}, is converted into the corresponding maximum plasma frequency, f_{peo}, for display. The results of all pulses taken from a single FORTÉ pass are combined to be plotted together as functions of FORTÉ latitude. Examples of data taken on three FORTÉ passes are shown in Figures. 4–6.

The first data plotted in each of Figures 4-6 are the latitude and longitude of the transmitter, T, and the path trajectory of the satellite, S. The dashed curves are the trajectories of puncture points for rays crossing at an altitude of 300 *km*, the approximate layer of peak plasma density. The great circle path from the transmitter to the footprint of FORTÉ, P, is plotted in Figures 4-6. As P becomes larger, ray bending due to refraction between ionospheric layers contributes more to the nonlinear increase in time lag, τ. Such ray bending effects are not easily modeled in moment expansion codes but are incorporated directly in the present layered ionosphere model.

Parabolic curves are fit to the numerical results for f_{peo}, T, and vertical TEC. Figure 4 represents a good example of FORTÉ data points consistent with one another and with the IRI. The plot of TEC is fit closely by a parabolic curve, showing a negative gradient as a function of latitude and small curvature. As expected, the scatter in f_{peo} and T is greater than that of TEC, but still on the order of 10%. For the point of closest approach of FORTÉ to the LAPP, f_{peo} taken from FORTÉ is 11.5 *MHz* and the corresponding value from the IRI above the LAPP is 12.2 MHz. Meanwhile the respective values for TEC are $5.3\times10^{17}\ m^{-3}$ and $5.4\times10^{17}\ m^{-3}$. Here both parameters show good agreement. Figure 5 shows FORTÉ data with less internal consistency and poorer agreement with the IRI. For the point of closest approach, f_{peo} taken from FORTÉ data is 6.1 *MHz* while that from the IRI is 8.8 *MHz*. The respective values for TEC are $1.7\times10^{17}\ m^{-3}$ and $3.2\times10^{17}\ m^{-3}$. Here the discrepancy between the FORTÉ TEC results and the IRI is nearly 50%. Also the TEC plot for FORTÉ shows a strong positive curvature, indicating a more complex functional relationship between TEC and latitude than seen in Figure 4. If indeed the FORTÉ results are accurate, there is a local ionospheric effect represented in Figure 5 that is not represented in the IRI. For Figure 6, FORTÉ results give f_{peo} = 9.8 *MHz* and TEC = $3.7\times10^{17}\ m^{-3}$, respectively within ~10% and ~20% of the IRI. Figure 6 differs from the IRI in that the latitudinal gradient given by the IRI is negative, while the gradients of f_{peo} and TEC in Figure 6 are positive.

Data taken at the points of closest approach in the 36 FORTÉ passes recorded are compared statistically with the IRI as follows. The average difference between f_{peo} obtained from FORTÉ and from the IRI is -1.8%, and the corresponding average difference for the TEC is -13%. Meanwhile, the root-mean-squared (rms) differences are 12% for f_{peo} and 21% for TEC. For the purposes of comparison, it is noted that f_{peo} obtained from FORTÉ shows a

rms variability from its mean of 28%, and the TEC data show a variability of 39%. For the same times and places in the IRI, the variability for f_{peo} is 22% and for TEC it is 29%. In addition to anticipated results, these data provide some new and unexpected insight. The FORTÉ results show more variability from the mean than the IRI. This is expected since the IRI can not represent the fine-scale detail obtained by direct local measurement; hence, it is a smoother, less variable function. Meanwhile, the rms discrepancies between the FORTÉ results and the IRI are about 9% less than the variability of the IRI itself. This is a good indication of a direct correlation between the FORTÉ and IRI results. It is surprising that agreement in f_{peo} between FORTÉ and the IRI is better than for the TEC. As explained above, f_{peo} is drawn from a higher moment of f_{peo}/f than is TEC, so one would normally expect the TEC to be more accurate. The precise cause of these unexpected results remains to be determined.

One may attempt to infer the accuracy of these FORTÉ results by observing the regularity of data with respect to a simple curve, such as the parabolas in Figures 4-6 or even straight line fits. The idea here is that ionospheric parameters might not be expected to fluctuate greatly along the observation path seen in a FORTÉ pass. Indeed, in the FORTÉ passes analyzed, the TEC fits parabolas to ~1.5% standard deviation and straight lines to ~2.8%. Meanwhile, f_{peo} fits parabolas to ~2.8% and straight lines to ~3.5%, while the corresponding figures for T are ~6.5% and ~7.5% respectively. An analysis of the least-squares fitting procedure used here indicates that f_{peo} and T should be expected to have ~2 and ~4 times respectively more scatter in the results than the TEC. This occurs because the time lag has a stronger dependence on TEC than upon the separated variables f_{peo} and T (Wolberg, 1967, Eq. (3.10.40)). It was noted above that the time lag for a vertical ray path from transmitter to satellite only exhibits nonlinearities due to terms in the index of refraction, and the most additional information expected is the second moment of N_e. Perhaps there is information in addition to the separation of f_{peo} and T as a result of refractive effects in inclined ray paths. For example, such effects might contribute to the quadratic terms in the f_{peo}, T, and TEC plots in Figures 4-6. The development of such conjectures requires considerably more work in modeling the latitudinal gradients of electron density and a refinement of the vertical profile modeling.

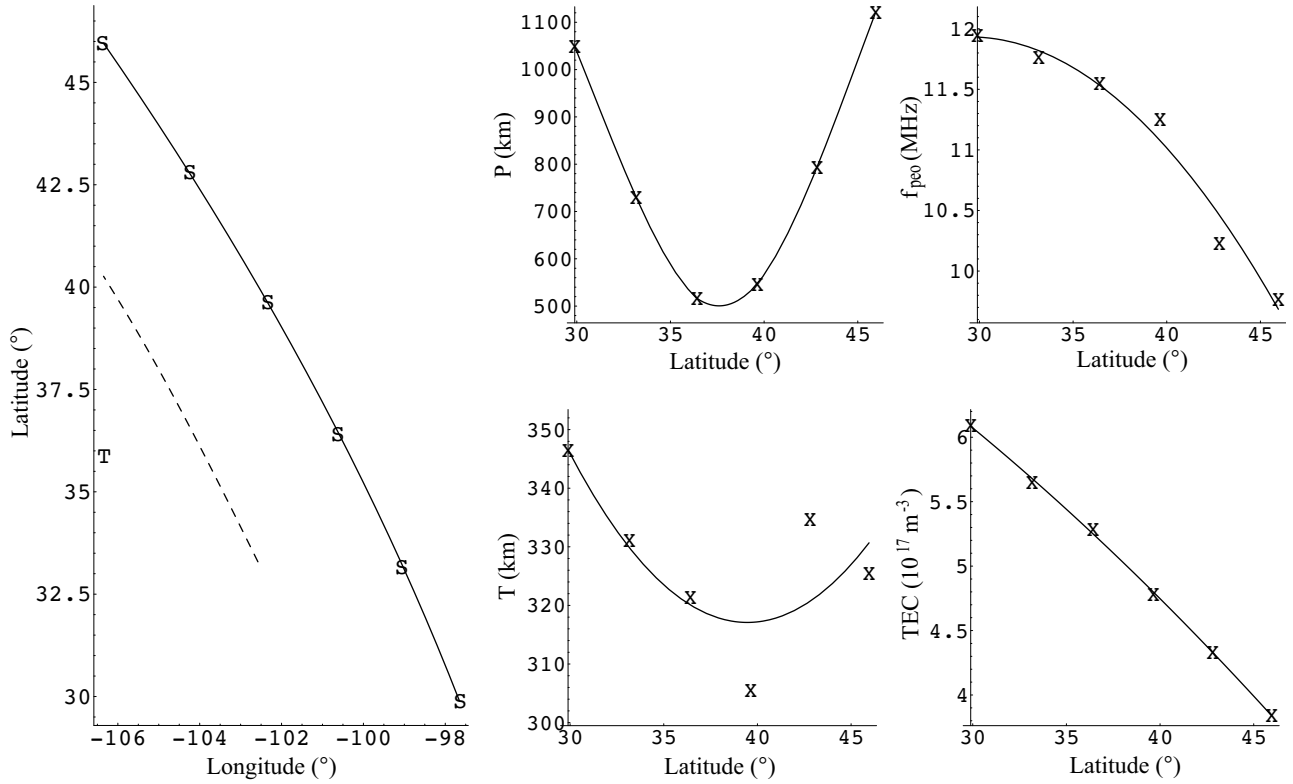

Fig. 4. Model fits to FORTÉ data from LAPP transmissions on March 27, 2001, at ~20:33 *UT*. Latitude and longitude are shown on a single plot for the transmitter, T, and satellite position, S, at each pulse. The dashed plot represents the puncture point of transmitter to satellite ray paths at an altitude of 300 *km*, the approximate layer of peak electron density. In the remaining four plots, data points marked by "X" represent separate LAPP pulses with the independent variable being FORTÉ latitude. The function *P* represents the great circle path length from the LAPP to the footprint beneath FORTÉ. The peak plasma frequency, f_{peo}; ionospheric thickness, *T*; and total vertical electron content, TEC, are shown separately. Solid parabolic curves are fit to the f_{peo}, *T*, and TEC.

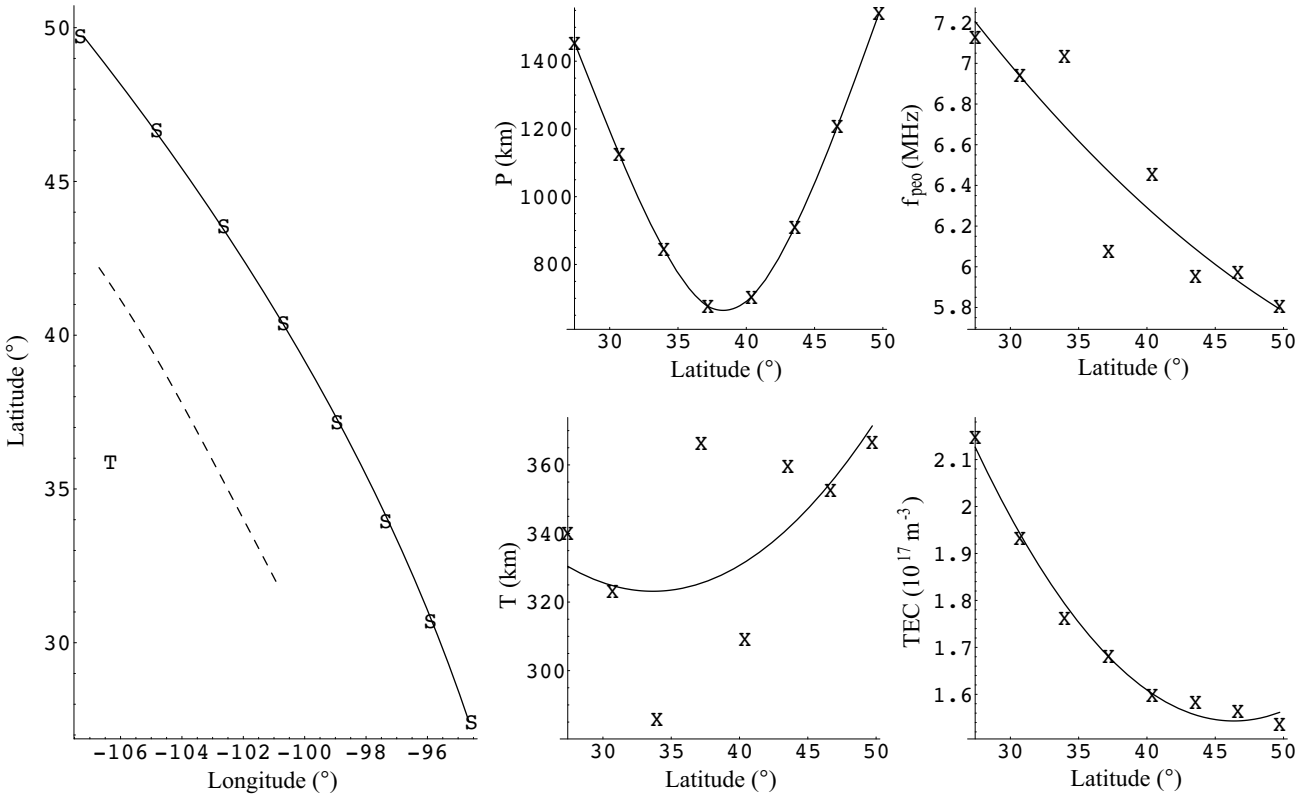

Fig. 5. Model fits to FORTÉ data from LAPP transmissions on July 26, 2001, at ~18:22 *UT*. This example shows FORTÉ results in TEC and f_{peo} considerably lower than those given by the IRI.

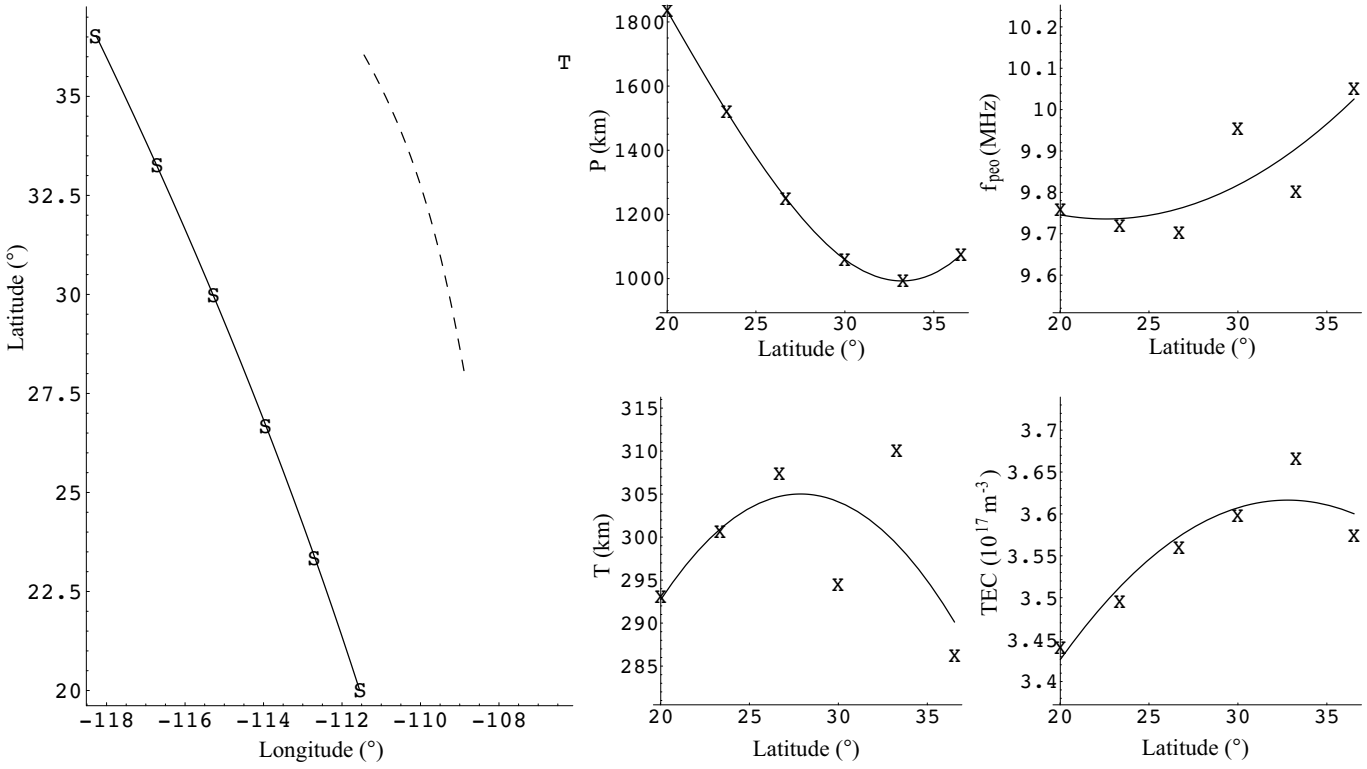

Fig. 6. Model fits to FORTÉ data from LAPP transmissions on April 27, 2001, at ~15:06 *UT*. This example shows FORTÉ results with a positive latitudinal gradient in TEC, contrary to the results of the IRI.

SUMMARY AND DISCUSSION

The capacity to extract significant additional information from trans-ionospheric pulse propagation has been enhanced by the present work. It has been known for some time that the frequency-dependent time lag for trans-ionospheric pulses is linearly dependent on the first moment of electron density between transmitter and receiver, TEC; and there is dependence on higher moments due to nonlinearities in the index of refraction and refractive effects. The computer code developed here is an advanced model of a layered ionosphere, based on the International Reference Ionosphere, which incorporates the empirically obtained International Reference Geomagnetic Field. The computer model serves as an "inversion" code through which one can extract peak electron density and ionospheric thickness in addition to TEC from empirically obtained data. This procedure is demonstrated using data gathered by the FORTÉ satellite.

The techniques developed here appear to work well; nevertheless, it is difficult to establish a detailed statement of precision for the results without complementary *in situ* data. In view of extracting the most in ionospheric parameters, the layered ionospheric model will be refined to consider latitudinal gradients and a coordinated fit of parameters through multiple pulses.

ACKNOWLEDGEMENTS

We would like to express our appreciation to the FORTÉ operations team, led by Phil Klingner and Diane Roussel-Dupre for their extensive support of this effort, and to David Smith and Daniel Holden for operation of the LAPP facility. We especially want to thank Ms. Amy Bartlett for her work in digitizing the FORTÉ data presented in this paper. This work was performed under the auspices of the United States Department of Energy.

REFERENCES

Argo, P., T. J. Fitzgerald, and R. Carlos, NICARE I HF propagation experiment results and interpretation, *Radio Sci.*, **27**, #2, 289-305, 1992.

Barton, C. E., International Reference Geomagnetic Field: the seventh generation, *J. Geomag. Geoelectr.*, **49**, 121-146, (1997).

Bilitza, D., "*International Reference Ionosphere 1990*," NSSDC/WDC-A-R&S 90-92. (1990).

Bilitza, D. and R. Williamson, Towards a better representation of the IRI topside based on Isis and Alouette data, *Adv. Space Res.* **25,** #1, 149-152 (1999)

Budden, K. G., *The propagation of radio waves, The theory of radio waves of low power in the ionosphere and magnetosphere*, Cambridge University Press; Cambridge, New York, New Rochelle, Melbourne, and Sydney (1988).

Heise, S, N. Jakowski, A. Wehrenphennig, Ch. Reigber, and H. Luhr, *Geophys. Res. Lett.*, **29**, 44-1 - 4-4 (2002).

Jacobson, A.R., S.O. Knox, R. Franz, and D.C. Enemark, FORTE observations of lightning radio-frequency signatures: Capabilities and basic results, *Radio Sci.*, *34* (2), 337, 1999.

Kelley, M. C., *The Earth's Ionosphere Plasma Physics and Electrodynamics*, Academic Press, San Diego and London (1989).

Massey, R.S., S.O. Knox, R.C. Franz, D.N. Holden, and C.T. Rhodes, Measurements of transionospheric radio propagation parameters using the FORTE satellite, *Radio Sci.*, *33* (6), 1739-1753, 1998.

Moses, R. W. and A. R. Jacobson, American Geophysical Union 2001 Fall Meeting, San Francisco, 12/10/01-12/14/01.

Myre, W., private communication, (June, 2002).

Roussel-Dupre, R. A., A. R. Jacobson, and L. A. Triplett, Analysis of FORTÉ data to extract ionospheric parameters, *Radio Science, 36* (6) 1615-1630 (2001).

Wolberg J. R., *Predicition Analysis*, D. Van Nostrand Co., Inc. Princeton, Toronto, London, Belbourn (1967).

E-mail address of R. W. Moses rmoses@lanl.gov